Multi-Feature Based Multiple Landmine Detection Using Ground Penetration Radar

Suncheol PARK, Kangwook KIM, Kwang Hee KO

School of Mechatronics, Gwangju Inst. of Science and Technology, 261 Cheomdangwagiro, Bukgu, Gwangju, Republic of Korea

withstar@gist.ac.kr, mkkim@gist.ac.kr, khko@gist.ac.kr

Abstract. *This paper presents a novel method for detection of multiple landmines using a ground penetrating radar (GPR). Conventional algorithms mainly focus on detection of a single landmine, which cannot linearly extend to the multiple landmine case. The proposed algorithm is composed of four steps; estimation of the number of multiple objects buried in the ground, isolation of each object, feature extraction and detection of landmines. The number of objects in the GPR signal is estimated by using the energy projection method. Then signals for the objects are extracted by using the symmetry filtering method. Each signal is then processed for features, which are given as input to the support vector machine (SVM) for landmine detection. Three landmines buried in various ground conditions are considered for the test of the proposed method. They demonstrate that the proposed method can successfully detect multiple landmines.*

Keywords

Ground Penetrating Radar, landmine detection, Support Vector Machine, PCA, geometric feature, multiple landmine.

1. Introduction

Safe landmine removal is an urgent but difficult job faced by many countries. The removal process requires detection of a landmine buried in the ground. Once it is detected, the landmine can be eliminated in various ways. Therefore, robust landmine detection is a key step in landmine removal.

Many efforts have been made for developing methods for detecting landmines. Among them, detection using a ground penetrating radar (GPR) has attracted many researchers' attention due to its various advantages over other devices; it can be used to detect landmines of metal and nonmetal materials [1] without changing its configuration. Moreover, it can be made small and portable such that it is used in various forms such as a stand-alone handheld sensor [2]-[6], a complementary sensor or a vehicle-mounted system in the form of an array of multiple antenna elements [7]-[9].

Detection of a landmine from a GPR signal requires extracting features of a landmine from the signal. There are various ways for computing features from the GPR signal for landmine detection such as geometrical feature of a landmine signal [10], hidden Markov models (HMMs) [6], Spatial Features analysis [11], polynomial fitting [12], texture-feature coding method (TFCM) [13], time-frequency features [14], [15], and principal component analysis (PCA) [16]-[18]. In [14], [17] and [18], multiple features for a landmine such as PCA and Fourier coefficients are used for robust detection and identification. Those methods are designed to detect a single landmine from the GPR signal with some clutters. However, they are not intended to handle the case that multiple landmines are captured in one signal set. More than one landmine may be buried in the ground, yielding a GPR signal containing multiple landmines. In this situation, the methods for single landmine detection are not able to operate properly if the signal is provided as input without *a priori* knowledge on the number of landmines in the signal. It might happen that only one landmine might be detected, and the others would be ignored as obstacles when the number of landmines in the signal is not known. Although the implication of this problem is profound, little research on this problem has been presented in the literature.

In this work, the problem of multiple landmine detection using the GPR is addressed, and a novel method is proposed, which detects multiple landmines from a GPR signal. The GPR scans a ground, to generate a signal. Next, the number of objects in the signal that are determined to be possible landmines is estimated. Once the number is computed, regions corresponding to each object are extracted, each of which is then processed to obtain features. The features are then used to decide if the objects are landmines or not. The decision is made using a support vector machine scheme (SVM). If a landmine is detected, its type (anti-personal and anti-tanks) is retrieved.

This paper contains two contributions. The first one is the segmentation procedure of each landmine from an input signal that may contain multiple landmines. Most of the landmine detection algorithms in the literature present methods for detection of a landmine from an input signal, which is usually assumed to contain at most one landmine. Therefore, without knowing the number of landmines in the signal, there is a high chance that landmines can be left undetected when the number of landmines in the signal is more than two. This problem can be handled after the number of landmines is computed. Here, the number can be estimated through segmentation, which has not been actively discussed in the literature so far. In this paper, our emphasis was laid on the segmentation of landmine signals and estimation of the number of landmines in the signal. Once the number of landmines is computed, then, identification of each landmine is performed. As a second contribution, the landmine identification method has been improved compared with our previous work [17] and [18]. In particular, SVM was employed for identification, which provided better results than the authors' previous method.

The paper is structured as follows. In Section 2, the overall procedure of multiple landmine detection is proposed to provide a workflow of the method. In Section 3, each step of the procedure is presented in detail. Examples are presented in Section 4 to demonstrate the potential of the proposed method. Section 5 concludes this paper with future work.

2. Overall Procedure

The overall procedure of multiple landmine detection is proposed as shown in Fig. 1. It consists of two major processes: segmentation and identification. The segmentation, which is indicated in a dotted rectangle in Fig. 1, estimates the number of possible landmines in GPR data. This step is important in the multiple landmine detection because it defines how many times the identification should be performed. Once the number of possible landmines is estimated, each segmented signal is processed for extracting features for identification. The identification, which is indicated in a black rectangle in Fig. 1, contains processes of signal extraction, post-processing of signal and feature extraction. Once the features of each signal are computed, identification of the signal is performed.

The first step is to normalize a GPR signal in order to minimize the influence that might be caused by the difference of the hardware and the individual experimental environments. Next, the number of objects in the signal is estimated using the energy projection method [17]. Once the number is estimated, signals for each individual object are extracted separately using the Symmetry Filtering Method [20]. The extracted object signals are processed using the envelope detector [21] and Gaussian filter to reduce noise and ground effects. Then features such as the principal components and geometric features (ratios and lengths of signatures in the signal) are computed for each signal, and then provided as input to the identification module. The identification of the input signal is made using the support vector machine (SVM) based on the features.

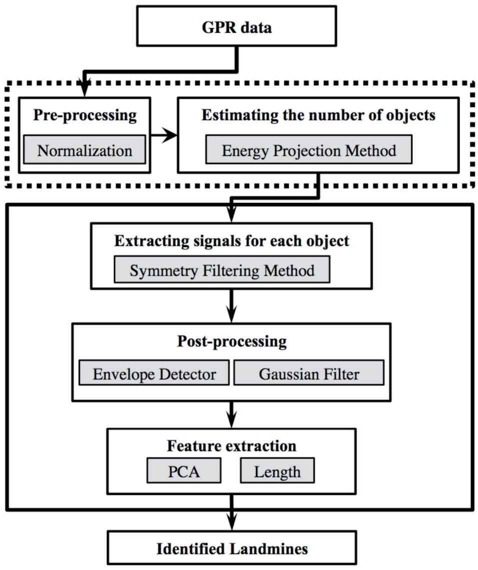

Fig. 1. The overall procedure of the proposed method.

3. Multiple Landmine Detection Algorithm

3.1 Pre-processing of GPR Signal

A GPR signal is given as a set of intensity values at x and y positions as shown in Fig. 2. Here, the x axis indicates the integer index of each sampling position (denoted as Column No.) for the width of the scanning area. The sampling interval of the two adjacent scanning positions is 15 mm. The y axis is the depth and the z axis is the strength of the signal. The strength of the GPR signal reflects the size and material type of a landmine in the ground. Therefore, it could be considered as a feature of a landmine. However, the strength can also be influenced by other factors such as the power of the GPR, the installation height of the radar and the properties of the ground. Therefore, the power intensities of B-scan signal are normalized for the strength in order to minimize such effects. The normalization is performed in a linear manner so that the strength of each signal is scaled to the range from zero to one.

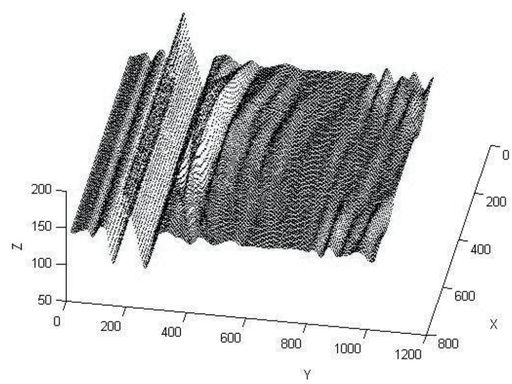

Fig. 2. An example of a GPR signal in 3D space.

3.2 Estimation of the Number of Objects

Estimation of the number of objects in the GPR signal mainly consists of three steps: removal of clutters, noise reduction and estimation of the number of objects. Assume that I is a GPR signal given as an image as shown in Fig. 3, where the strength of the signal is given as intensity values in the x-y (Column No. and Depth) plane.

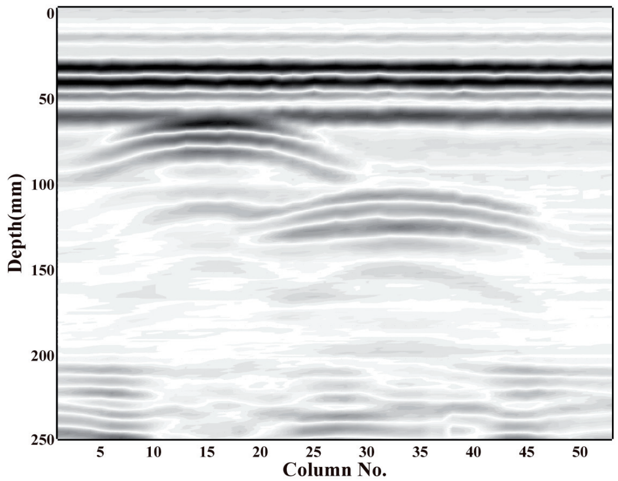

Fig. 3. An example of an input signal given as an image in gray scale. The clutter due to the ground is clearly indicated.

Clutters in the signal are removed from I using the average subtraction method [22], to yield I_c. The method is effective in removing the reflection from the ground, which is nearly constant in strength. It works as follows. $I(x,y)$ is an intensity of the signal at x and y. Then, the new $I_c(x,y)$, which is obtained by using the average subtraction method, is

$$I_c(x,y) = I(x,y) - \underset{For\,\forall x}{E}[I(x,y)]\,. \tag{1}$$

Here, $E_x[]$ indicates the operator computing the average for all x at y_i. This equation is applied at each y_i. Fig. 4(a) shows an example of the signal I_c. It clearly shows that most of the ground reflection has been removed. Then, a 3 by 3 Gaussian mean filter with the sigma of 0.5

$$f(x,y) = \frac{1}{2\pi\sigma^2} e^{-\frac{x^2+y^2}{2\sigma^2}} \tag{2}$$

is applied to the signal I_c for noise reduction, yielding the signal I_{cs} of Fig. 4. Next, the Sobel edge detector [23] is applied to the signal I_{cs} in order to extract signatures. The detector is an algorithm to extract edges in an image using the gradient of the intensity distribution. Given the input intensity $I = I(x,y)$, the magnitude of the gradient is

$$\nabla I_M = mag(\nabla I) = \sqrt{\left(\frac{\partial I}{\partial x}\right)^2 + \left(\frac{\partial I}{\partial y}\right)^2}\,. \tag{3}$$

If it is larger than or equal to a threshold, the intensity is set to one. Otherwise, it is set to zero. The threshold needs to be determined through various experiments. An example of the extracted edges is given in Fig. 4(c). The edges are then projected onto the y-z and x-z planes, respectively. During the projection, the intensity values at the same projected positions are accumulated to produce the accumulated projected signatures in the y-z and x-z planes. As demonstrated in Fig. 4(d), the projected values form distinct groups. Then, the numbers of groups whose peaks are larger than a tolerance T_2 in each of the y-z and x-z planes are counted to be n_{y2} and n_{x2}. Next, among n_{y2} and n_{x2}, the numbers of groups, which have ranges (widths) wider than a tolerance T_1, are computed to be n_{y1} and n_{x1}. The largest one between n_{y1} and n_{x1} is selected to be the number of objects in the signal, which is denoted by n_{obj}. This estimation procedure is called Energy projection method [19]. Figure 4(d) shows that two objects are detected.

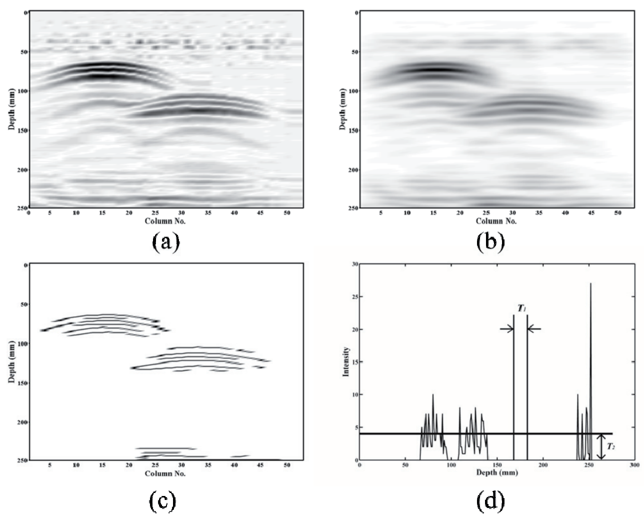

Fig. 4. The results of the steps of the energy projection method. (a) The result of removing the constant clutter. (b) The result of applying the Gaussian filter. (c) The result of applying the Sobel edge detector. (d) The result of projecting GPR data to *y-z (depth and intensity)* plane.

T_1 is the minimum width of the signal range in the projection planes. T_2 is the minimum intensity in the GPR data. Signals either with narrower width than T_1 or with intensity smaller than T_2 are ignored as noise. Basically, these values need to be chosen empirically with various landmines and objects. However, a guideline for the choice is that they should be so selected that the estimated number of objects in the signal becomes more than the actual number of landmines. In this case objects other than landmines can be discarded in the decision step. This way, the possibility that a landmine is missed, a dangerous case than the false alarm, can be minimized.

3.3 Extracting Individual Objects

When an object buried in the ground is scanned by a GPR, a symmetric parabolic shape is obtained as shown in Fig. 4(a).

Therefore, using a filter, which extracts a symmetric shape, a signal corresponding to the object in the ground can be obtained. The symmetry filtering method [20] can be used to handle this problem. The GPR data in this work are given as shown in Fig. 2. Then, the method can be applied as follows. First, the symmetry position in the signal is located using the following equation.

$$I_2(x,y) = \sum_{m=-M}^{M} \sum_{k=1}^{K} I(x-k, y-m) I(x+k, y-m) . \quad (4)$$

Here, M and K are variables related with the radar pulse and the valid aperture of the radar given in [20]. I is the intensity, and the values of x and y are the column number and the depth, respectively. Next, the range direction symmetry weighting matrix is computed using the following equation.

$$I_3(y) = \frac{\sum_{m=-M}^{M} \sum_{k=1}^{K} I(x_0-k, y-m) I(x_0+k, y-m)}{\sqrt{(\sum_{m=-M}^{M} \sum_{k=1}^{K} I(x_0-k, y-m)^2)(\sum_{m=-M}^{M} \sum_{k=1}^{K} I(x_0+k, y-m)^2)}}$$
$$x_0 = \operatorname{argmax}(I_2(x,y)) \quad (5)$$

The function, argmax($I_2(x,y)$), returns x coordinate, x_0, where I_2 in (4) is maximum. After that, the lateral direction symmetry weighting matrix is computed by

$$I_4(x_0-x,y) = I_4(x_0+x,y) = \frac{\sum_{m=-M}^{M} \sum_{n=-N}^{N} I(x_0-x-n, y-m) I(x_0+x+n, y-m)}{\sqrt{(\sum_{m=-M}^{M} \sum_{n=-N}^{N} I(x_0-x-n, y-m)^2)(\sum_{m=-M}^{M} \sum_{n=-N}^{N} I(x_0+x+n, y-m)^2)}} . \quad (6)$$

Once I_3 and I_4 are obtained, the synthetic symmetry filtering weighting matrix is computed by

$$I_5(x,y) = e^{\gamma I_{3n}(y)} e^{\mu I_{4n}(x,y)} . \quad (7)$$

Here, γ and μ are the range and lateral reduction factors and set to one in this work. $I_{3n}(y)$ and $I_{4n}(x,y)$ are the normalized $I_3(y)$ and $I_4(x,y)$. The symmetric shape I_6 is then extracted by multiplying the input signal I by I_5.

$$I_6(x,y) = I(x,y) I_5(x,y) . \quad (8)$$

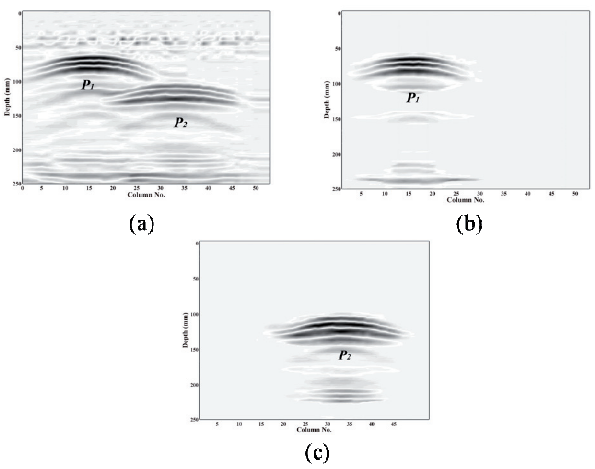

Fig. 5. The results of the symmetry filtering method. (a) shows input data containing two symmetric patterns, P_1 and P_2. (b) is the result showing one symmetric pattern, P_1. (c) is the result of the other symmetric pattern, P_2 after P_1 has been removed.

Consider a GPR signal as shown in Fig. 5(a), where the clutter has been reduced and the number of objects has been estimated by using the procedure in Section 3.2. Next, the symmetry filtering method is employed to extract one symmetric pattern. The method detects the strongest signal in the data and extracts the associated symmetric pattern. As an example, the left one in Fig. 5(a) is extracted, which is denoted as P_1. The pattern is then subtracted from Fig. 5(a), to produce a signal without P_1, which is shown in Fig. 5(c). If the number of objects is estimated to be n_{obj}, this process is repeated n_{obj}-1 times to yield n_{obj} signal sets, containing the symmetric patterns of each object.

3.4 Post-processing

Each extracted signal is processed to further reduce noise for feature extraction. A GPR signal changes its sign with respect to zero, due to the property of an electromagnetic wave. Such alternation is eliminated for the subsequent process using the Envelope Detection Method [21], which restores the original signal from those modulated in a high frequency. The detector is given by

$$y_{(n)} = f_1 x_{(n)} + f_2 y_{(n-1)} e^{-\tau} . \quad (9)$$

Here,

$$f_1 = \begin{cases} 1 & \text{if } x_{(n)} \geq y_{(n-1)} e^{-\tau} \\ 0 & \text{otherwise} \end{cases}$$
$$f_2 = \begin{cases} 1 & \text{if } x_{(n)} < y_{(n-1)} e^{-\tau} \\ 0 & \text{otherwise} \end{cases} \quad (10)$$

where $x_{(n)}$ is the n-th input signal, $y_{(n)}$ is the extracted envelope at position n and τ is the reduction rate. The reduction rate needs to be selected such that the envelope detector yields the best result. A large τ could reduce the effect of the envelope detector. On the other hand, a small τ may distort the original signal. In order to avoid such problems, a GPR frequency is considered such that the power of the signal reduces to half. Namely, an equation $e^{-\tau x} = 0.5$ is derived. From this equation, τ can be selected so that x becomes equal to the GPR frequency. $y_{(0)}$ is defined to be zero because a signal containing an object will not start at the beginning of the GPR signal. In other words, the distance between the GPR and an object is larger than zero.

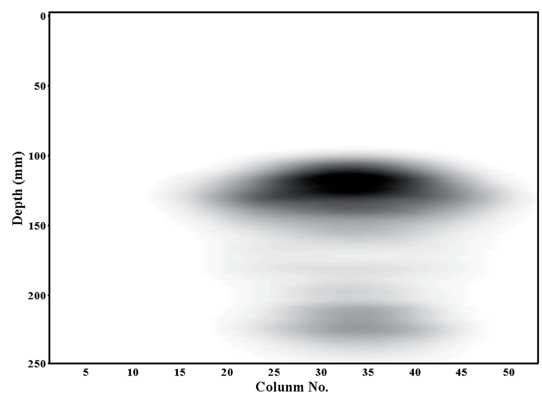

Fig. 6. The result of Gaussian processed data.

Next, a Gaussian filter is applied in order to reduce high frequency noise in the signal. For this work, a Gaussian filter with a 3 by 3 window and the sigma of 0.5 is used. The result of the filtered signal is shown in Fig. 6. Next, for better feature extraction, the filtered signal is processed such that the intensity values, which are less than 50% of the maximum intensity in the signal, are set to zero. The result of this step is given in Fig. 7.

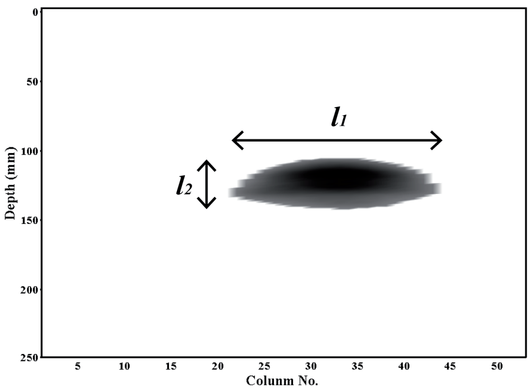

Fig. 7. The result of applying the threshold.

3.5 Extracting Features of an Object

The post-processed signal is used to extract features of a landmine for identification. First, normalization of the signal is performed to consider the difference of the reflected power along the burial depth. The maximum and the minimum intensity values of the signal are scaled linearly to the range of 0 to 1, to adjust the power difference due to the different depths.

Two geometric features and one statistical feature are considered. The two geometric features are the geometric dimensions of the signal intensity distribution as shown in Fig. 7. In the *x*-*y* (Column No. and Depth) plane, intensity values larger than 50% of the maximum of the intensity usually leave an elliptic shape as shown in Fig. 7, which is obtained in the post-processing step given in Section 3.4. The shape can be characterized with the horizontal size and the vertical length. As a first feature the size, l_1 is measured along the horizontal axis as shown in Fig. 7. It is related with the size of an object reflected in the signal. The bigger an object is, the larger l_1 becomes. This feature can_differentiate objects with respect to their size. This value is measured as the number of columns that the horizontal size of the region covers. The second feature is the length, l_2, which is measured along the depth (y axis) in the figure. It is mainly dependent on permittivity and permeability of materials of an object. The radio wave transmittance is different according to the object materials. It is observed that the length l_2 of a plastic object is longer than that of a metallic one. Therefore, this feature can separate a steel object from a plastic one. This feature is measured in mm.

As a third feature, a principal component by the principal component analysis (PCA) method is used. PCA method analyzes discrete data points in n-dimensional space, producing n principal components in n principal directions, forming n pairs of the component value and its corresponding direction. Each component represents a pattern of the data in that direction. The PCA has been frequently used in the context of detection, and its applicability can be extended to clutter reduction [24].

Consider m sets of data, $\Gamma_i = (x_{1i}, x_{2i}, \ldots, x_{ni})$, $i = 1, \ldots, m$ in n-dimensional space. The average data of the m data sets are obtained by

$$\Phi = \frac{1}{m}\sum_{i=1}^{m}\Gamma_i \,. \tag{11}$$

The difference of Γ_i with Φ is computed by $\phi_i = \Gamma_i - \Phi$. Then the covariance of the data sets is then

$$\mathbf{C}_\Phi = \frac{1}{(m-1)}\sum_{i=1}^{m}\varphi_i\varphi_i^T \,. \tag{12}$$

The eigenvectors and eigenvalues of the covariance matrix are the principal components, which are computed by solving the following equation.

$$\mathbf{C}_\Phi \mathbf{u} = \lambda \mathbf{u} \,. \tag{13}$$

Here, $\mathbf{u}$ and λ are a vector and a scalar value, respectively. $\mathbf{u}$ and λ satisfying (13) are the eigenvectors and their eigenvalues of the covariance matrix, serving as the principal components of the data.

A GPR signal is given in 3D space as shown in Fig. 2. The intensity distribution can be obtained by projecting the signal in the *x*-*z* and *y*-*z* planes. Among them, the intensity distribution of the signal projected onto the *x*-*z* (column no. vs. intensity) plane is selected because it shows clearer features of each landmine. An example of this projection is given in Fig. 8. Then, PCA is applied to the projected signal to obtain two principal components and their corresponding direction vectors as depicted in Fig. 8.

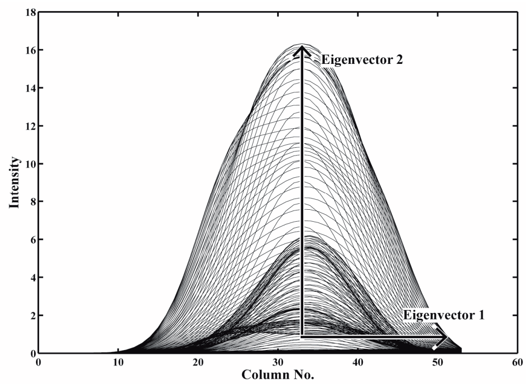

Fig. 8. The result of the projected GPR signal onto *x*-*z* plane used in the projection step.

In this work, the direction close to the x axis happens to correspond to the largest covariance value because most of the signal values are clustered near the x axis in the *x*-*z* plane when the signal is projected on the plane. The eigenvectors are not suitable for features of an object because the signal patterns are almost symmetric so that they do not show any difference. The eigenvalue of Eigenvector 1 is not appropriate as a feature because most of the signal strengths are clustered near the *x* axis, making the eigenvector directed in the same axis. The eigenvalue of Eigenvector 2, however, captures the reflection patterns of an object, which depend on materials and the size of the object.

3.6 Landmine Identification

Landmine identification is performed by comparing features computed in Section 3.5 with those in a database that contains features of various landmines buried in different ground conditions. If a match is found in the database, then the input landmine is identified. There are a lot of algorithms for identification such as the hidden Markov models [6], Mahalanobis distance based method [14], the decision tree [25], Bayesian learning [25] and Supporting Vector Machine (SVM) [25]. Among them, SVM is chosen in this work. It is a machine-learning algorithm used for data identification. A database is constructed, which contains features extracted from existing data sets. The features are classified into several groups, the outer most boundary elements of which are used to create optimal hyper planes differentiating each group. Algorithms for computing such hyper planes and robust decision are the main components of SVM. Once such a database is available, decision can be made that a group is determined where the features of input data belong. Various SVMs' are introduced in the related literature. In this work, a method using the radial basic function (RBF) is employed [26].

The basic concept of SVM is presented as follows. Suppose that there exist various data groups, which can be distinguished from each other. SVM is an algorithm to determine the optimal boundaries of the data groups for the group classification. Consider there are two groups of data, *A* and *B*. Here, the circles are the data in Group *A*, and the triangles are the data in Group *B*.

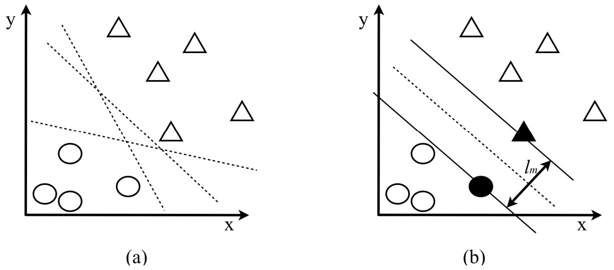

Fig. 9. An example of SVM. (a) shows two data groups with various separating boundaries. (b) shows an optimal hyper plane separating the two groups. Here, l_m is the maximum margin.

As shown in Fig. 9(a), an infinite number of boundaries can be introduced to separate the two groups. SVM selects one boundary that can optimally represent the boundaries of each group as illustrated in Fig. 9(b). In Fig. 9(b), the dotted line is the optimal separating line, called the optimal hyper plane, which is determined in such a way that the distance between the two data groups becomes maximal, or the maximum margin, l_m, becomes maximal. In general, SVM can be formulated as follows.

Consider that there exist data $\mathbf{D}_s$ in *p* dimensions.

$$\mathbf{D}_s = \left\{(\mathbf{x}_i, y_i) \mid \mathbf{x}_i \in \mathbf{R}^p, y_i \in \{-1,1\}, i = 1,\cdots,n_p\right\}. \quad (14)$$

Here, $\mathbf{x}_i$ is a vector in $\mathbf{R}^p$, n_p is the number of data, and y_i is the vector class. The hyper plane of this data set is obtained by solving the optimization problem:

$$\begin{aligned} &\min_{w,\xi} \frac{1}{2}\mathbf{wx} + C\sum_{i=1}^{l}\xi_i \\ &\text{subject to}: \\ &y_i(\mathbf{wx}_i + b) \geq 1 - \xi_i, i = 1,\cdots,l. \end{aligned} \quad (15)$$

Here, $\mathbf{w}^T$ is the normal vector of a hyper plane, $\mathbf{x}$ is the input data set, ξ is a slack variable and *C* is a constant for providing a constraint to Lagrange multipliers. Given the sign function,

$$\operatorname{sgn}(s) = \begin{cases} -1, s < 0 \\ \ \ 0, \ s = 0 \\ \ \ 1, \ s > 0 \end{cases} \quad (16)$$

a decision function using the hyper plane for determination of a data class is given as:

$$f(\mathbf{x}) = \operatorname{sgn}(\mathbf{wx} + b)\,. \quad (17)$$

In this work, three features are considered as discussed in Section 3.5. Each feature corresponds to one axis, forming 3D feature space. Therefore, one object is represented as one point in the feature space as shown in Fig. 10. As illustrated in the figure, a landmine buried in the ground of different conditions and at various depths forms a cluster in the space. These data are provided as input to SVM for constructing a database. Later, given a point in the space, detection of the point is performed using the database. In order to determine if an object is a landmine or not, the three feature values for objects other

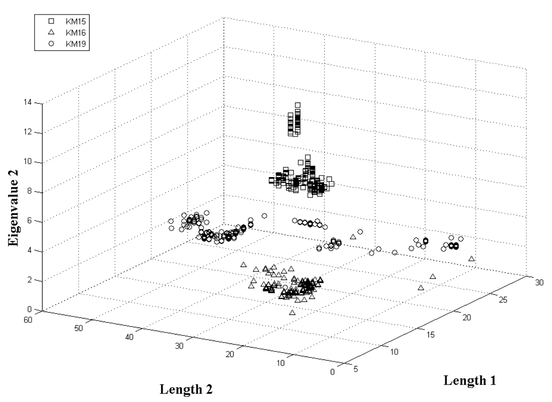

Fig. 10. A plot of features of three landmines buried in dry sand.

than landmines, so called clutters, are added to the database to form groups for non-landmines. Various rocks different in size or plastic and metal cans can be processed for this purpose. The database needs to be updated to contain features of various objects, which would increase the identification rate for landmines.

3.7 Implementation

The proposed method was implemented using a PC of 2.7 GHz CPU and 8 Gbyte RAM. The operating system of the computer was Windows 7, and Visual C++ and Matlab were used for implementation.

Conceptually the proposed method consists of six primary modules, modules for pre-processing, estimating the number of objects, extracting objects' signals, post-processing, extracting features and identification. Each primary module consists of one or more functions. The pre-processing module contains a function for normalization. The module for estimation of the number of objects contains a function of the energy projection method. The module for signal extraction provides a function of the symmetry filtering method. The post-processing module is composed of two functions: envelope detection and Gaussian filter. The feature extraction module consists of three functions of computing PCA and geometric lengths. The theoretical basis of these functions is given in Section 3.5. The identification module contains a function of SVM for identification as given in Section 3.6. The actual implementation of the method is structured as shown in Fig. 11. There exists a function for file I/O and data handling. This is a core part of the implementation, based on which the functions for processing GPR signals and identification are implemented. The functions have interfaces with the file I/O and data handling for input and output. The sequence of execution of the functions is managed by the file I/O and data handling function.

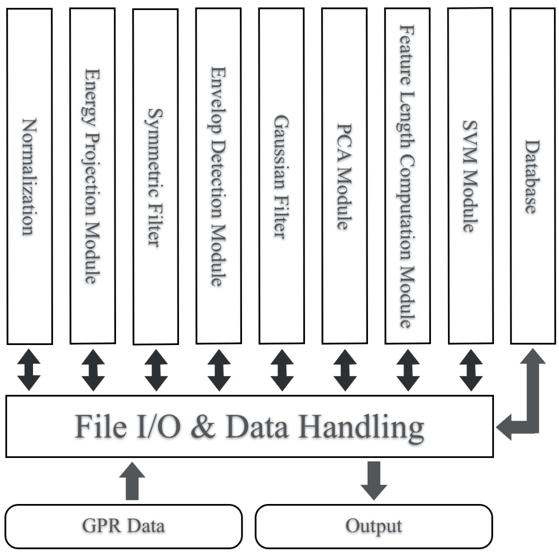

Fig. 11. A schematic diagram of the implemented program.

4. Experiments

In this work, three landmines are considered as shown in Fig. 12; KM16, which is made of steel, is an anti-personnel landmine. KM15 and KM19 are anti-tank landmines, each of which is made of steel and plastic, respectively. Three different ground materials (sand, soil, and gravel) are considered with three moisture levels (dry, medium, and wet).

(a) (b) (c)

Fig. 12. The landmines used in the experiments. (a) KM15, (b) KM16, (c) KM19.

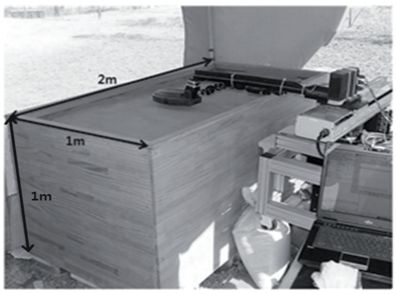

Fig. 13. The setup for the experiments.

For the experiments, a GPR system of Minehound VMR2 from COBHAM is used. The GPR is attached to an arm, which moves horizontally. A landmine is buried in a wooden box of 1 m × 2 m × 1 m, which is filled with sand, soil or gravel of three moisture levels. The configuration for the experiments is shown in Fig. 13.

The method for estimation of the number of buried objects is tested with the three landmines. For this test, three test cases are considered: (1) Case 1: KM16 and KM19 buried at 10 cm and 30 cm in the dry sand, (2) Case 2: KM15, KM19 and KM16 buried at 10 cm, 30 cm and 20 cm in the dry sand, (3) Case 3: KM16 and KM15 buried at 10 cm and 30 cm in the dry sand. The three cases, Cases 1, 2, and 3, are depicted in Fig. 14. The threshold values T_1 and T_2 are selected to be 13 mm and 5% of the largest power in the signal for the estimation.

The projection images of Case1 to *y-z* and *x-z* planes are shown in Fig. 15. Here, the projection data in *y-z* plane show three signal groups. The first one from the left corresponds to the surface reflection, which is to be removed. On the other hand, the data in *x-z* plane show one distribution pattern. Therefore, in this case, the projection data in *y-z* plane are selected for the estimation of the number of objects. Here, two islands are observed in the data of *y-z* plane, which has been successfully estimated by the energy projection method. The correct numbers of objects were also obtained for Cases 2 and 3 using the proposed method.

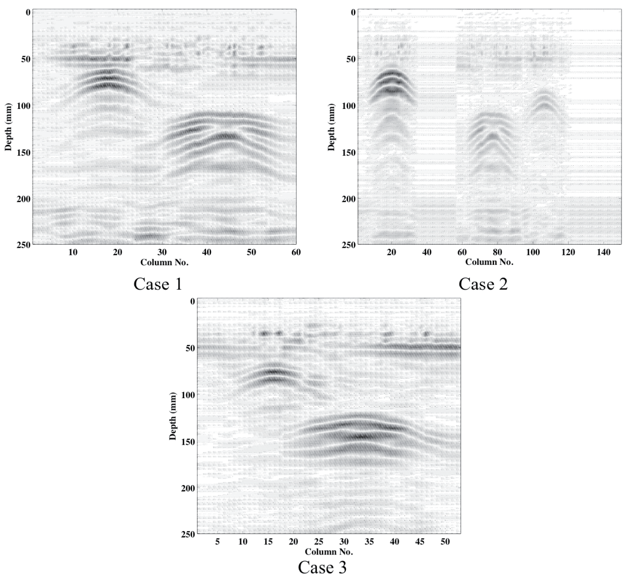

Fig. 14. Input signals for the test cases.

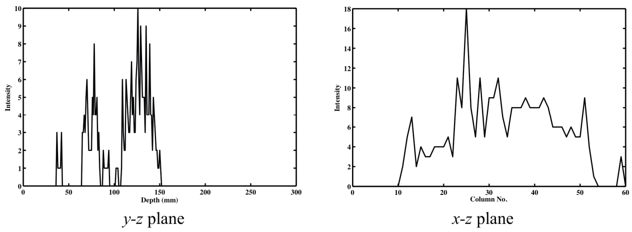

Fig. 15. The projection images of Case 1 to *y-z* and *x-z* planes.

Next, the identification process is demonstrated with various examples. A database is created using the three landmines buried in different conditions as summarized in Tab. 1. In total, 162 cases are considered. Each case is produced by averaging measurements of three separate scans of the case. For each case three features are computed and stored in the database with their corresponding landmine information.

Landmine types	KM15, KM16, KM19
Ground conditions	dry, medium, wet
Ground types	sand, gravel, soil
Burial depths (cm)	5, 10, 15, 20, 25, 30

Tab. 1. Types of landmines and burial conditions for construction of the database.

In order to simulate real signals, input signals are prepared adding various levels of Gaussian noise. The noise model used in these experiments employs a random function with normal distribution, whose probability distribution function is

$$pdf(x) = \frac{1}{\sqrt{2\pi\sigma^2}} e^{\frac{-x^2}{2\sigma^2}}. \tag{18}$$

with $\sigma = 0.5$. The noise created by this model is added after scaling its magnitude to be from 0 to 50% to the original signal. An example of an input signal is shown in Fig. 16(a). Here, the case of KM16 buried at 10 cm in dry sand is taken. The image in Fig. 16(a) is the original one, and the rest images Figs. 16(b), (c) and (d) show those with 10%, 30% and 50% noise added, respectively. It is obvious that as the noise level grows, the pattern of the signal becomes less clear.

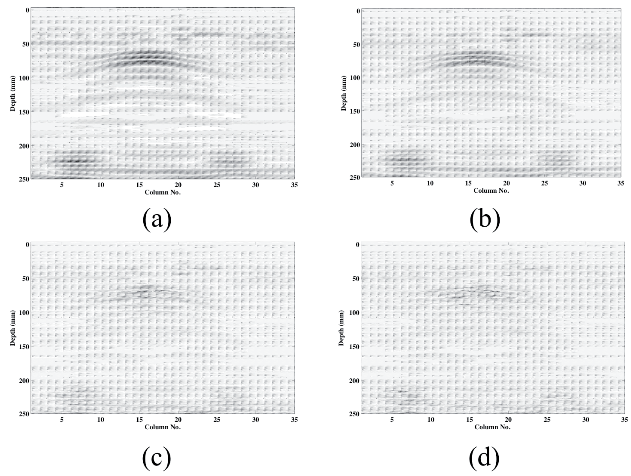

Fig. 16. Example data with various levels of Gaussian noise added. (a) no noise, (b) 10%, (c) 30% and (d) 50%.

The input cases for experiments are prepared as follows. Three ground types, three moisture levels, six burial depths, and three landmines are considered. Moreover, the number of noise levels is five. Therefore, the total number of combinations becomes 810.

Fig. 17 is a graph showing the changes of identification rates of the input cases with respect to the levels of noise added to the signal, the ground conditions and different burial depths. In order to show the changing patterns of the identification rates, the results of the identification of each case are arranged with respect to the five noise levels, the three ground types and the three moisture levels. The identification rates of the three landmines and six burial depths are averaged. For example, consider 'saw1' case. It indicates the dry sand ground condition. The average identification rates for three landmines buried at six burial depths are computed for each noise level, which are plotted with respect to the noise level. The other eight cases are similarly processed to produce graphs as shown in Fig. 17. The plot does not show the difference of identification rate of each landmine for different burial depths. However, it can show how the identification rates change with respect to the noise level depending on the ground conditions.

The highest identification rates are obtained with 10% of noise, which gradually decrease as the level of noise increases. For sand (saw1, saw2, and saw3), the detection rate is more than 98% irrespective of the moisture level. For soil (sow1, sow2, and sow3), the rate is decreased. However, it still shows more than 90%. For the gravel ground (grw1, grw2, and grw3), the detection rate is more than 95%, but it decreases as the moisture level is increased.

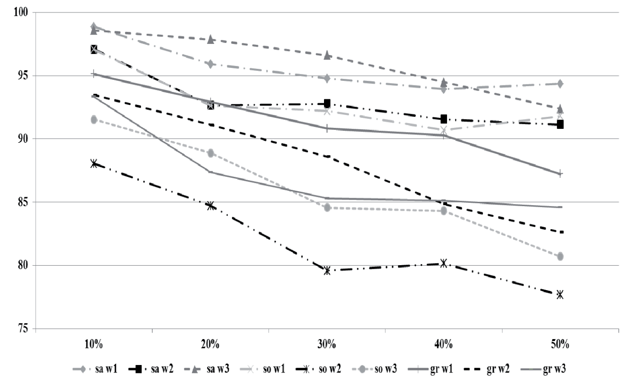

Fig. 17. The changes of the detection rate with respect to the noise level. 'sa', 'so' and 'gr' indicate sand, soil and gravel. 'w1', 'w2', and 'w3' are the moisture levels of dry, medium and wet. The horizontal and vertical axes are the noise and the detection rates, respectively.

5. Conclusions

This paper proposes a novel method for detecting multiple landmines buried in the ground of various conditions using a GPR. The method consists of clutter reduction, estimation of the number of objects in the GPR data, isolation of object signals, feature extraction and detection. The tests show that the proposed method can mostly detect multiple landmines in various conditions.

The proposed method has two limitations: choice of tolerances and database construction. The method requires a couple of user-defined values: threshold values for the estimation of the number of objects and a parametric value used by the symmetry filtering method. These values mainly depend on the properties of the GPR hardware used in the system and are critical in the process. The other limitation is that a database for landmines and various other foreign objects should be constructed for robust detection. The database for non-landmines could be limited in that it cannot consider all possible clutters different in size, shape and material. It means that there might be a false-alarm case that a non-landmine object is determined as a landmine due to the limited amount of data in the database. These two limitations can be overcome through extensive experiments with objects and landmines.

The overall procedure of the method is designed for general environments. However, the tests in the paper were performed in controlled conditions, and the tolerances were chosen and the database was constructed for those conditions. Therefore, it is necessary to refine the tolerances and to improve the database by considering more realistic situations. A thorough evaluation of the method for selection of tolerances and enhancing the database using real field data is recommended for future work.

Acknowledgements

This work was supported in part by the Korea Evaluation Institute of Industrial Technology (10041950).

References

[1] MACDONALD, J., LOCKWOOD, J. R., MCFEE, J., ALTSHULER, T., BROACH, T., CARIN, L., HARMON, R., RAPPAPORT, C., SCOTT, W., WEAVER, R. *Alternatives for Landmine Detection*. Rand Corporation, 2003.

[2] AMAZEEN, C. A., LOCKE, M. C. Developmental status of the U.S. Army's new handheld standoff mine detection system (HSTAMIDS). In *Second International Conference on Detection of Abandoned Land Mines, 1998.* (Conf. Publ. No. 458). Edinburgh (England), 1998, p. 193-197.

[3] HO, K. C., GADER, P. D. A linear prediction land mine detection algorithm for hand held ground penetrating radar. *IEEE Transactions on Geoscience and Remote Sensing*, 2002, vol. 40, no. 6, p. 1374-1384.

[4] VAN DER MERWE, A., GUPTA, J. A novel signal processing technique for clutter reduction in GPR measurements of small, shallow land mines. *IEEE Transactions on Geoscience and Remote Sensing*, 2000, vol. 38, no. 6, p. 2627-2637.

[5] NISHIMOTO, M., UENO, S., KIMURA, Y. Feature extraction from GPR data for identification of landmine-like objects under rough ground surface. *Journal of Electromagnetic Waves and Applications*, 2006, vol. 20, no. 12, p. 1577-1586.

[6] GADER, P. D., MYSTKOWSKY, M., ZHAO, Y. Landmine detection with ground penetration radar using hidden Markov models. *IEEE Transactions on Geoscience and Remote Sensing*, 2011, vol. 39, no. 6, p. 1231-1244.

[7] SATO, M., KOBAYASHI, T., TAKAHASHI, K., FUJIWARA, J., FENG, X. Vehicle mounted SAR-GPR and its evaluation. In *Proceedings of SPIE*. Orlando (U.S.A.), 2006, vol. 6217.

[8] HARMON, R. S., HOLLOWAY, J. H., BROACH, J. T. Processing of GPR data from NIITEK landmine detection system. In *Proceedings of SPIE*. Maryland (U.S.A.), 2003, vol. 5089.

[9] YAROVOY, A., SAVELYEV, T., ZHUGE, X., AUBRY, P., LIGTHART, L., SCHAVEMAKER, J., TETTELAAR, P., DEN BREEJEN, E. Performance of UWB array-based radar sensor in a multi-sensor vehicle-based suit for landmine detection. In *Radar Conference EuRAD 2008.* Amsterdam (The Netherlands), 2008, p. 288-291.

[10] NATH, B., BHUIYAN, A. A geometrical feature based sensor fusion model of GPR and IR for detection and classification of anti-personnel mines. In *Proc. of the 7th Internat. Conf. on Intelligent Systems Design and Applications ISDA '07.* 2007, p. 849-856.

[11] HUANG, X., ZHANG, L., LI, P. Classification and extraction of spatial features in urban areas using high-resolution multispectral imagery. *IEEE Geoscience and Remote Sensing Letters*, 2007, vol. 4, no. 2, p. 260-264.

[12] ZHU, Q., COLLINS, L. M. Application of feature extraction methods for landmine detection using the Wichmann/Niitek ground-penetrating radar. *IEEE Transactions on Geoscience and Remote Sensing*, 2005, vol. 43, no. 1, p. 81-85.

[13] TORRIONE, P., COLLINS, L. M. Texture features for antitank landmine detection using ground penetrating radar. *IEEE Transactions on Geoscience and Remote Sensing*, 2007, vol. 45, no. 2, p. 2374-2382.

[14] SAVELYEV, T. G., VAN KEMPEN, L., SAHLI, H., SACHS, J., SATO, M. Investigation of time-frequency features for GPR landmine discrimination. *IEEE Transactions on Geoscience and Remote Sensing*, 2007, vol. 45, no. 1, p. 118-129.

[15] SUN, Y., LI, J. Time-frequency analysis for plastic landmine detection via forward-looking ground penetrating radar. In *IEE Proceedings, Radar, Sonar and Navigation*, 2003, vol. 150, no. 4, p. 253-261.

[16] HUANG, C. W., LEE, K. C. Application of ICA technique to PCA based radar target recognition. *Progress in Electromagnetics Research*, 2010, vol. 105, p. 157-1870.

[17] KO, K. H., JANG, G., PARK, K., KIM, K. GPR-based landmine detection and identification using multiple features. *International Journal of Antennas and Propagation*, 2012, vol. 2012, p. 1-7.

[18] PARK, K., PARK, S., KIM, K., KO, K. H. Multi-feature based detection of landmines using ground penetrating radar. *Progress in Electromagnetics Research*, 2013, vol. 134, p. 455-474.

[19] PARK, S., KIM, K., KO, K. H. Multiple landmine detection algorithm using ground penetrating radar. In *International Geoscience and Remote Sensing Symposium (IGARSS 2012)*. Munich (Germany), 2012, p. 3190-3193.

[20] LI, T., KONG, L., ZHOU, Z. Symmetry filtering method for GPR clutter reduction. In *International Conference on Microwave and Millimeter Wave Technology (ICMMT 2008)*. 2008, p. 1515-1517.

[21] FRITSCH, C., IBANEZ, A., PARRILLA, M. A digital envelope detection filter for real-time operation. *IEEE Trans. on Instrumentation and Measurement,* 1999, vol. 48, no. 6, p. 1287 to 1293.

[22] ABUJARAD, F., JOSTINGMEIER, A., OMAR, A. A. Clutter removal for landmine using different signal processing techniques. In *Proceedings of the Tenth International Conference Ground Penetrating Radar*. Delft (The Netherlands), 2004, p. 697-700.

[23] GONZALEZ, R. C., WOODS, R. E. *Digital Image Processing 2/E*. Upper Saddle River, NJ: Prentice Hall, 2002.

[24] KABOUREK, V., CERNY, P., MAZANEK, M. Clutter reduction based on principal component analysis technique for hidden objects detection. *Radioengineering*, 2012, vol. 21, no. 1, p. 464-470.

[25] MITCHELL, T. M. *Machine Learning*. Boston, MA: McGraw-Hill, 1997.

[26] CRISTIANINI, N., TAYLOR, J. S. *An Introduction to Support Vector Machines and Other Kernel-based Learning Methods*. Cambridge University Press, 2000.

About Authors ...

Suncheol PARK was born in Seoul, Republic of Korea. He received a B.S. degree in Electrical Engineering from Ajou University, Korea, in 2011. He is currently an MS student at Gwangju Institute of Science and Technology, Gwangju, Korea. His current research interest includes machine learning, signal processing and landmine detection and identification.

Kangwook KIM was born in Mokpo, Republic of Korea. He received a B.S. degree in Electrical Engineering from Ajou University, Korea, in 1997, and M.S. and Ph.D. degrees in Electrical and Computer Engineering from the Georgia Institute of Technology, GA, USA, in 2001 and 2003, respectively. His Ph.D. research was on the design, analysis, and measurement of pulse-radiating antennas. From 1999 to 2003, he participated in research on ultra-wideband, pulse-radiating antenna as a graduate research assistant, and from 2003 to 2005, he participated in multi-modal landmine detection system research at the Georgia Institute of Technology as a postdoctoral fellow. From 2005 to 2006, he was with the Samsung Advanced Institute of Technology. He joined the faculty of the Gwangju Institute of Science and Technology in 2006 as an assistant professor. His current research interests include electrically small antennas, remote sensing of concealed objects, and ultra-wideband electromagnetics.

Kwang Hee KO was born in Seoul, Republic of Korea. He received a B.S degree in Naval Architecture and Ocean Engineering from Seoul National University in 1995, M.S. degrees in Mechanical and Ocean Engineering in 2001 and a Ph.D. degree in Ocean Engineering from the Massachusetts Institute of Technology (MIT), Cambridge, MA, USA, in 2003. His research interests include feature matching, landmine detection, geometric modeling, CAD/CAM and computer graphics. He worked as a postdoctoral associate at MIT from 2003 to 2004 and as a research associate at the Design and Manufacturing Institute, Stevens Institute of Technology, Hoboken, NJ, from 2004 to 2005. He joined the School of Mechatronics, Gwangju Institute of Science and Technology, Gwangju, Korea, in 2006 and worked as an assistant professor until 2010. He is currently an associate professor at Gwangju Institute of Science and Technology, Gwangju, Korea.